Investigating Link- and Network-level Bicycle Traffic Flow Characteristics using a Microsimulation Approach

Ying-Chuan Ni*[1], Michail Makridis[1], and Anastasios Kouvelas[1]

[1]Institute for Transport Planning and Systems, Swiss Federal Institute of Technology (ETH) Zurich, Switzerland

Short summary

Implementing cycling infrastructure for road users has become a popular transport policy for cities to create a sustainable urban environment nowadays. A thorough understanding of bicycle traffic is required to evaluate new infrastructure designs. To fill the remaining knowledge gap in this aspect, this study aims to investigate bicycle traffic flow characteristics on dedicated bike lanes. A microsimulation tool is used to simulate various scenarios and compute bicycle traffic states. From the simulation results, bicycle flow characteristics presented at both link and network levels are identified and discussed. The findings are expected to be applied to future research regarding large-scale bicycle traffic flow modeling.
Keywords: Bicycle flow; Dedicated bike lane; Fundamental diagram; Macroscopic fundamental diagram; Microscopic traffic simulation; None-lane-based traffic

1 Introduction

Cities have been planning to expand dedicated cycling infrastructure over urban areas to enhance the usage of this active transport mode and foster a more sustainable transport environment (Pucher & Buehler, 2017). In E-Bike City project, we aim to allocate around 50% of the existing urban road space to cyclists and other slow modes (D-BAUG ETH Zurich, 2022). It is envisioned that cycling will become a primary transport mode in the city. Therefore, urban transport systems need to be re-designed to meet the growing cycling demand. However, traffic and transport modeling nowadays often regards cycling as a auxiliary mode and ignores its congestion dynamics. An in-depth and universal understanding of bicycle traffic flow characteristics is still lacking, which hinders the planning for quality cycling infrastructure.

In fact, there were plenty of studies which focused on bicycle traffic flow in the past decades. At microscopic level, bicycle flow was often simulated by cellular automata (CA), which is a simple discrete time and space model (Gould & Karner, 2009; Jiang et al., 2004). Although there has been much research endeavor attempting to overcome its discrete space limitation by introducing various extensions, CA still fails to account for the large behavioral heterogeneity nature of bicycle flow. There were also studies developing social force models which can better consider the two-dimensionality of cycling motion (Liang et al., 2018; Zhao & Zhang, 2017). However, they were known to be too computationally expensive for large-scale modeling purposes. Twaddle et al. (2014) provided a thorough review and comparison of different bicycle modeling approaches. On the other hand, microsimulation tools seem to be a good option which lies between these two types of approaches. Grigoropoulos et al. (2021) used SUMO to simulate the traffic performance of a bicycle route in various scenarios. Nevertheless, SUMO simulates bicycles through its built-in sublane function, which divides a bike lane into multiple sublanes for overtaking (Lopez et al., 2018). The suitability of this setup in simulating bicycle traffic is questioned.

There were studies which investigated bicycle traffic flow with empirical data. By performing a series of experiments, Wierbos (2021) analyzed the macroscopic bicycle flow properties, including capacity, capacity drop, jam density, and queue discharge rate in different scenarios, such as narrowing bottleneck, merging, and queuing at a stop line. However, the flow performance at congested states was not reported. Through field observation, Li et al. (2015) constructed FDs for bicycle-only paths with the presence of bottlenecks. It was found that bicycle traffic can maintain a relatively high flow rate even when the density is larger than the critical density, which was

different from the simulation results of the CA studies. However, the conclusion was based on an arbitrary curve-fitting. There was no detailed description regarding the empirical observation after the hypothetical critical density. Guo et al. (2021) also plotted FDs for the wide ring-shaped track bicycle flow experiments they conducted. A similar trend that a constant flow rate remains across a certain region of densities was discovered. It was inferred that this phenomenon was resulted from the staggered formation of bicycles at high density situations which allowed the lateral space to be utilized more efficiently. Therefore, the flow rate would not start decreasing right from the onset of congestion. Still, we remain skeptical about the outcome of such effect on FDs since (1) only few data points were generated in the study and (2) the FDs only specifically described the traffic states of small wide ring-shaped track experiments, which might be very different from the real-world cycling environment. More detailed explanations and reflection about the observed phenomena are required. Hence, the FDs of dedicated bike lanes are yet to be explored.

At the network-level, the macroscopic fundamental diagram (MFD) of a bike lane network is of interest. Little research effort has shed light on MFD for bicycle traffic in particular. Huang et al. (2021) used empirical data to investigate the impact of bicycle flow and infrastructure design on the shape of car MFD. Loder et al. (2021) first intended to capture the tri-modal interactions by using multi-modal MFDs for each mode. The bicycle MFD was generated and fitted with empirical data following the same method proposed for car MFD without careful consideration for the unique bicycle flow properties. Later on, Huang et al. (2022) applied the concept of 3D-MFD on car-bicycle traffic. Both empirical data and Vissim simulation were adopted to generate MFDs. However, there was no specific discussion on the shape and properties of the resulting bicycle MFD. To a certain extent, these studies still focused on the mixed car-bicycle traffic flow on urban roads. Besides, they were based on scarce and heterogeneous bicycle flow data collected in the field. A basic understanding of MFD for a dedicated bike lane network is still lacking.

To allocate more dedicated road space to bicycles considering its congestion dynamics within an urban network, the aggregated bicycle traffic needs to be precisely described. FD and MFD are two proper ways to model the network traffic performance. Hence, this study seeks to investigate the characteristics of bicycle traffic flow by generating its FDs and MFDs.

2 Methodology

This section first describes the selection of microsimulation tool and the calibration of bicycle-related simulation parameters. In the second part, the simulation environments and output analysis methods are explained.

As mentioned in section 1, empirical bicycle flow data containing complete traffic states are still lacking. Therefore, instead of relying on empirical data, a microsimulation approach is adopted in this study to investigate bicycle traffic characteristics at the aggregated level. Among all the traffic simulation tool, PTV Vissim is believed to possess the most sophisticated bicycle simulation function, which is not a simple projection of car traffic (PTV Group, 2023).

Compared to car driving behavior, tactical-level decisions play an even bigger role in cycling motion. In addition, bicycle traffic is not regulated by lane markings, which makes it more complex. Vissim outperforms other simulation tools by including a built-in lateral model, which enables it to simulate the special features of none-lane-based traffic, such as the overtaking behavior of two-wheelers. Moreover, the diamond queue function represents the cyclists by a diamond shape and makes the queue configuration more realistic, as pointed out in Gavriilidou et al. (2019). This also influences the resulting standstill (jam) density and queue discharge rate. Vissim also allows users to set the look ahead/back distance and number of interacting objects of each agent. This function is helpful for simulating road users, like cyclists, which have better anticipation ability.

Although there may still be several detailed cycling behavior features which are not presented in the bicycle simulation function in Vissim, it is hypothesized in this study that the function is sufficient to reproduce the bicycle traffic dynamics at aggregated levels. All the bicycle modeling parameters which need to be calibrated, including desired acceleration distribution, desired speed distribution, car-following model parameters, and lateral model parameters, follow the setup suggested in Kaths et al. (2021).

To plot bicycle flow FDs, eight 300-m-long dedicated bike lanes with three different lane widths, 1.5 m, 2 m, and 2.5 m, are built in Vissim. Bottlenecks are placed in the middle of lanes $4 \sim 8$ to generate congested situations. Two types of bottleneck are considered. The first type of bottleneck on lanes $4 \sim 6$ reduces the path width by 0.5 m, while the second is 1-m-wide on lanes $7 \sim 8$. Table 1 lists all the created bike lanes. The one-minute-aggregated density, speed, and flow data are obtained from a 10-m-long segment before the bottlenecks on these bicycle paths. A five-hour scenario with varying demand profile is implemented.

Table 1: Dedicated bike lanes for FD generation

Dedicated bike lane no.	Lane width (m)	Bottleneck width (m)
1	1.5	none
2	2.0	none
3	2.5	none
4	1.5	1.0
5	2.0	1.5
6	2.5	2.0
7	2.0	1.0
8	2.5	1.0

In addition to FDs, this study also aims to derive a bicycle flow MFD. An arterial with 2-m-wide bike paths in two directions on both sides of the road is built in Vissim. Six intersections divide the arterial into seven road sections. The green time at every intersection is 40 s, while the cycle time equals to 70 s. Each road link is 150 m long. Accordingly, the signal offset is set to 35 s. The average flow and density data are collected every five minutes from the ten road links in the middle, excluding the inflow and outflow links. A fifteen-hour scenario is designed to mimic the demand profile of a typical weekday, while the first half-an-hour is considered a warm-up period for the network to be filled up.

3 Results and discussion

This section describes the analyzed simulation results and research findings based on the results.

Bicycle flow fundamental diagrams

Figure 1 shows the density-flow FDs of bike paths with different widths. In order to compare the FDs of different lane widths in a convenient way, the density value is transformed into two-dimensional. The y-axis also becomes flow rate per 1-m-width so that it can align with the transformed density. By doing so, we keep the speed information (slope) meaningful.

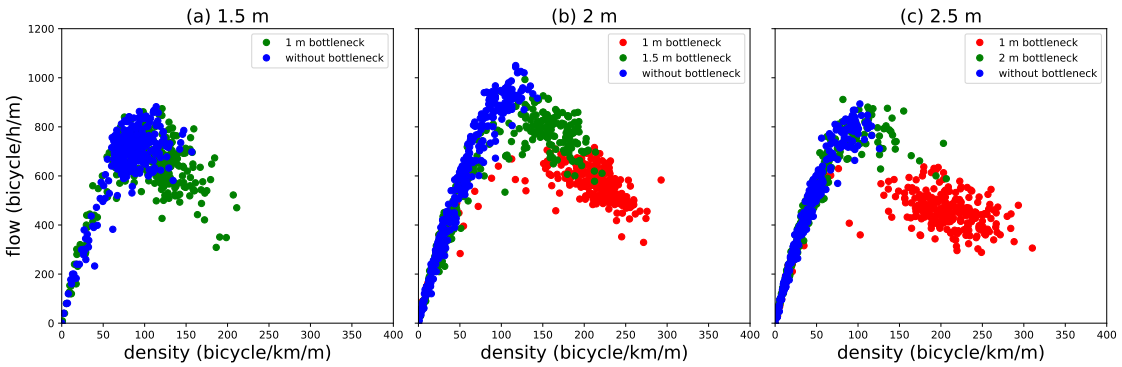

Figure 1: Flow-density FDs of bicycle flow on bike lanes with different lane widths

The effect of different lane widths can then be discussed. As can be seen in Figure 1a, few data points in the decreasing branch can be observed in the 1 m bottleneck case. Only little congestion effect is shown, which indicates that bicycle traffic flow on 1.5 m width does not have significant difference with the flow on 1 m width. Still, it implies that bicycles in free flow condition need more than 1-m-wide lane space to execute overtaking maneuvers. The narrowing bottleneck does impact the traffic volume. In addition, a large scatter of blue dots can also be observed near the critical density. This may be resulted from the stochastic stop-and-go disturbance caused by the desired speed heterogeneity.

Figure 1b plots the FD of the bicycle flow on 2-m-wide lane. Compared to the 1.5-m-wide lane, the capacity is increased, indicating that there are more overtaking behaviors. By looking at the blue dots in the free flow branch, one can see that it does not have the same large scatter near the critical density as shown in the 1.5-m-width case, indicating that a wider lane width can handle disturbance better. Furthermore, the green data points become more obvious in the decreasing branch. Even though the lane width reduction is the same, the congestion effect is more significant when the path width is 2 m before the bottleneck. This indicates that a 2-m-wide bicycle lane allows cyclists to utilize the existing lane space more efficiently. By looking at the red dots, one can also see that the capacity drop becomes more significant when the bottleneck is only 1 m wide, which is caused by the larger lane width narrowing.

The FD of the bicycle flow on 2.5-m-wide lane, as shown in Figure 1c, has a smaller capacity per unit lane width than the lane with 2 m width does, which seems to be non-intuitive. This means that widening the lane width does not necessarily increase the degree of lane space utilization. On the other hand, no obvious decreasing branch can be found in the case of the 2-m-wide bottleneck (green dots). These both indicate that the capacity of the bike lane with 2 m width is closer to the performance limit of dedicated bicycle infrastructure compared to the other two lane widths.

Table 2 summarizes the FD attributes of each lane width. Note that the free flow speed is not included here and will be discussed later. The capacity is determined by the point with the largest flow rate, while the critical density is the density of the capacity point. The jam density values are obtained by running simulations and placing a stop line on each lane. As can be seen in the table, the jam density values are different in cases of different lane widths, which also demonstrates the different degrees of lane space utilization.

Table 2: Shape attributes of FDs of bike lanes with different widths

	1.5 m width	2 m width	2.5 m width
Capacity (bicycle/h/m)	882.24	1049.91	893.53
Critical density (bicycle/km/m)	113.92	117.32	102.23
Jam density (bicycle/km/m)	408.00	460.50	410.8

To sum up, bicycle flow on 2-m-wide bike lane can utilize the lane space most efficiently. There is no improvement when widening the lane width to 2.5 m. This can also be understood by considering that the lateral space required by a cyclist is between 1 m and 1.3 m in the adopted Vissim setup.

Other than the difference between various lane widths, there are a few special characteristics of non-lane-based bicycle traffic flow regarding the free flow speed. As can be seen in Figure 2a, which is the speed-density FD of the bike lane with 2 m width in the case without bottleneck, the speed decreases rapidly as the density increases. This is the result of large desired speed heterogeneity. Bicycle flow is significantly slowed down by slow cyclists. Table 3 computes the average speed values in six divided density ranges. It is believed that this phenomenon is more significant in bicycle traffic than in car traffic. In addition to the speed heterogeneity, the effect of overtaking is another special characteristics of bicycle flow which was often overlooked. Figure 2b shows the results of a single-file bicycle traffic flow with no overtaking allowed. It can be observed that the speed decreases more rapidly as the density increases than in the case with overtaking. In the single-file case, cyclists loss the possibility to overtake slow cyclists, which further degrades the bicycle flow performance. Therefore, it is important to consider these two aspects when modeling bicycle traffic flow.

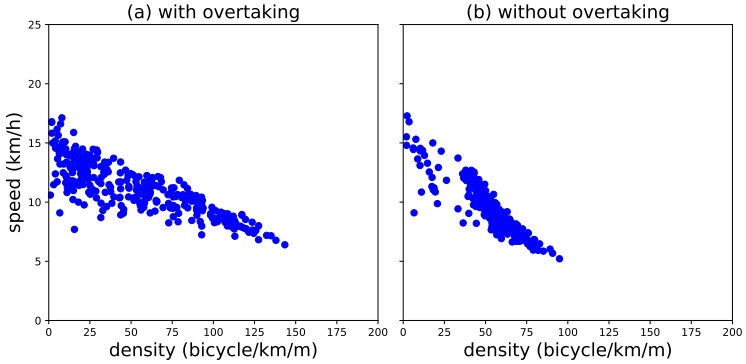

Figure 2: speed-density FDs of bicycle flow on a 2-m-wide bike lane (a) with overtaking (b) without overtaking

Table 3: Free flow speeds of bike lanes in six density ranges

Density (bicycle/km/m)	Average free flow speed (km/h)		
	1.5 m width	2 m width	2.5 m width
$0 \sim 25$	13.85	13.19	13.50
$25 \sim 50$	10.66	11.75	11.98
$50 \sim 75$	10.09	10.83	10.67
$75 \sim 100$	8.38	9.82	8.81
$100 \sim 125$	6.78	8.32	7.44
$125 \sim 150$	5.28	7.19	—

On the other ahnd, the existence of a constant flow branch around critical density pointed out by the previous studies cannot be observed from the FDs in Figure 1. It is suspected that the constant flow may actually stem from the better anticipation behavior of cyclists on the short ring-shaped track. The phenomenon may not appear in FDs of bike lanes in the real-world.

Bicycle flow macroscopic fundamental diagram

Figure 3 presents the MFD of the built bicycle lane arterial. The density variation is shown by the color of each data point. From the figure, one can observe an MFD curve with low scatter, showing the relationship between accumulation and network traffic performance can also be applied to bicycle flow. There are only few deviated data points which are caused by hysteresis, as shown by the color representing the normalized standard deviation of density. Since the simulation was carried out on a homogeneous arterial with equal link lengths and signal timing plans, no obvious decreasing branch can be observed.

The MFD is further analyzed by using the method of cuts (MoC) proposed by Daganzo and Geroliminis (2008). Each practical cut can be generated according to a moving observer speed and the number of blocks the observer can pass through γ. In the previous subsection, it was mentioned that the free flow speed varies a lot across different density values for bicycle flow. Therefore, this study modifies the MoC for bicycle traffic. The free flow speeds calculated in Table 3 are used to generate cuts. For each γ value, there is one corresponding speed. The saturation flow rate is determined by several Vissim simulation runs. Note that unlike typical car traffic, the maximum flow rates at a free flow lane segment and a stop line can be slightly different due to the staggered queue formation. No cuts in the decreasing branch are generated since there is no congested traffic state in the designed homogeneous arterial scenario. Figure 4 shows the cuts derived from the modified method. Compared to the examples which use only a single average speed value in Figure 5, the modified method produces more accurate cuts.

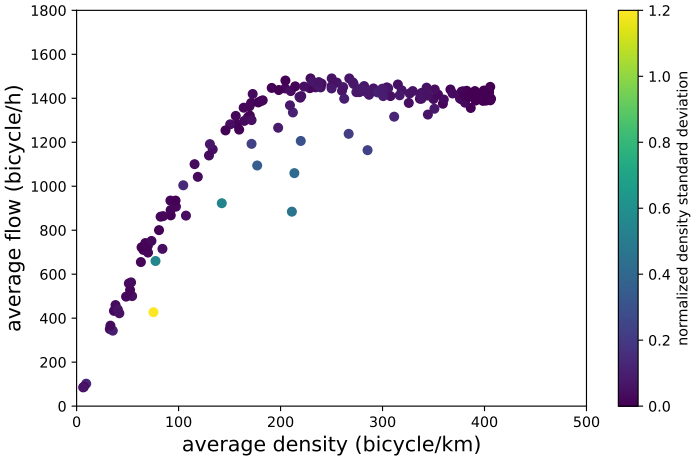

Figure 3: MFD of the bike lane arterial

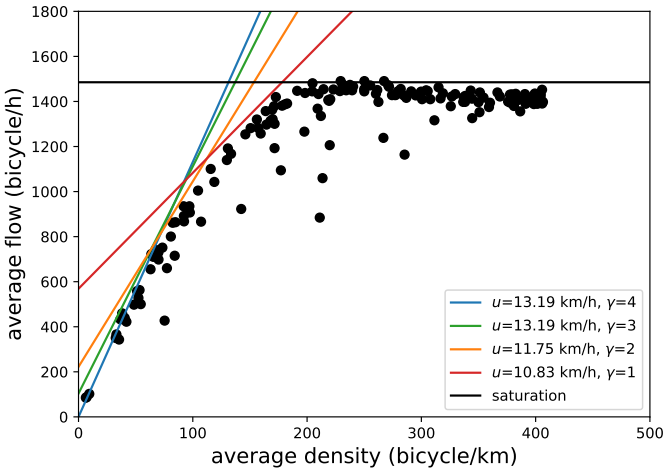

Figure 4: MFD of the bike lane arterial with cuts generated by the modified MoC

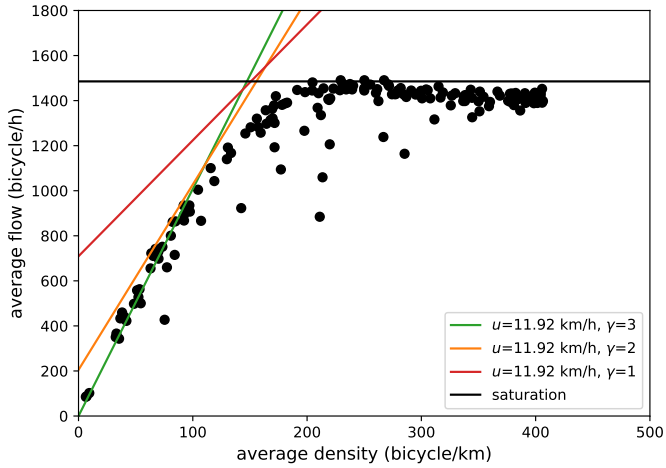

Figure 5: MFD of the bike lane arterial with cuts generated by a single speed value

In addition, a little decreasing trend can be observed after the critical density in the MFD although no spillback situation occurs in the simulated scenario. The decreased average flow rate may be the effect of anticipative cycling behavior. The speed of bicycles discharging from intersections decreases when there are too many queuing cyclists at the downstream links. This is a special phenomenon resulted from the look ahead behavior designed in Vissim. In this setup, cyclists look further downstream to determine their following speed.

4 Conclusions

This study investigates the characteristics of bicycle traffic flow on dedicated infrastructure by looking at FDs of different lane widths and an MFD of a bike lane arterial which are generated from microsimulation. The identified features are discussed and compared with the findings in the previous studies pertaining to bicycle flow modeling.

At link-level, it is found that lane widths greatly influences the FD attributes. A proper width can be found based on the lateral space required by a cyclist so that they can utilize the lane space in the most efficient manner. At free flow situations, the speed decreases as the density increases due to the desired speed heterogeneity. However, the overtaking behavior mitigates such effect by enabling bicycles to utilize the lateral space. On the other hand, the existence of a constant flow branch, which was pointed out in the previous ring-shaped track experiment, on real-world bike lanes is questioned.

This study also applies the MoC to derive the upper-bound MFD for bicycle traffic on dedicated infrastructure. To the best of our knowledge, this is the very first attempt to discuss bicycle MFD by using carefully-examined bicycle flow attributes. It is found that the modified method can better capture the shape of an MFD for none-lane-based bicycle traffic where the behavioral heterogeneity is large.

The results in this study largely depend on the setup in the microsimulation tool. Although the representativeness of the calibrated built-in bicycle simulation model may be argued, the overall macroscopic characteristics of bicycle flow observed from the FDs and MFD are deemed to be valid. The findings can be used for more complex network-wide bicycle traffic modeling, such as cell transmission model or MFD-based traffic assignment, and therefore assist dedicated cycling infrastructure planning by transport authorities which seek to increase bicycle usage.

Acknowledgements

This work was supported by E-Bike City project of the Department of Civil, Environmental and Geomatic Engineering at ETH Zurich.

References

Daganzo, C. F., & Geroliminis, N. (2008). An analytical approximation for the macroscopic fundamental diagram of urban traffic. *Transportation Research Part B: Methodological*, *42*(9), 771–781. https://doi.org/10.1016/j.trb.2008.06.008

D-BAUG ETH Zurich. (2022). E-Bike City: Designing sustainable streets. https://ebikecity.baug.ethz.ch/en/

Gavriilidou, A., Daamen, W., Yuan, Y., & Hoogendoorn, S. (2019). Modelling cyclist queue formation using a two-layer framework for operational cycling behaviour. *Transportation Research Part C: Emerging Technologies*, *105*, 468–484. https://doi.org/10.1016/j.trc.2019.06.012

Gould, G., & Karner, A. (2009). Modeling Bicycle Facility Operation. *Transportation Research Record: Journal of the Transportation Research Board*, *2140*(1), 157–164. https://doi.org/10.3141/2140-17

Grigoropoulos, G., Hosseini, S. A., Keler, A., Kaths, H., Spangler, M., Busch, F., & Bogenberger, K. (2021). Traffic Simulation Analysis of Bicycle Highways in Urban Areas. *Sustainability*, *13*(3), 1016. https://doi.org/10.3390/su13031016

Guo, N., Jiang, R., Wong, S., Hao, Q.-Y., Xue, S.-Q., & Hu, M.-B. (2021). Bicycle flow dynamics on wide roads: Experiments and simulation. *Transportation Research Part C: Emerging Technologies*, *125*, 103012. https://doi.org/10.1016/j.trc.2021.103012

Huang, Y., Sun, D., Li, A., & Axhausen, K. W. (2021). Impact of bicycle traffic on the macroscopic fundamental diagram: some empirical findings in Shanghai. *Transportmetrica A: Transport Science*, *17*(4), 1122–1149. https://doi.org/10.1080/23249935.2020.1832157

Huang, Y., Sun, D., & Zhang, S. (2022). Three-dimensional macroscopic fundamental diagram for car and bicycle heterogeneous traffic. *Transportmetrica B: Transport Dynamics*, *10*(1), 312–339. https://doi.org/10.1080/21680566.2021.1994050

Jiang, R., Jia, B., & Wu, Q.-S. (2004). Stochastic multi-value cellular automata models for bicycle flow. *Journal of Physics A: Mathematical and General*, *37*(6), 2063–2072. https://doi.org/10.1088/0305-4470/37/6/007

Kaths, H., Keler, A., & Bogenberger, K. (2021). Calibrating the Wiedemann 99 Car-Following Model for Bicycle Traffic. *Sustainability*, *13*(6), 3487. https://doi.org/10.3390/su13063487

Li, Z., Ye, M., Li, Z., & Du, M. (2015). Some Operational Features in Bicycle Traffic Flow. *Transportation Research Record: Journal of the Transportation Research Board*, *2520*(1), 18–24. https://doi.org/10.3141/2520-03

Liang, X., Xie, M., & Jia, X. (2018). New Microscopic Dynamic Model for Bicyclists' Riding Strategies. *Journal of Transportation Engineering, Part A: Systems*, *144*(8). https://doi.org/10.1061/JTEPBS.0000148

Loder, A., Bressan, L., Wierbos, M. J., Becker, H., Emmonds, A., Obee, M., Knoop, V. L., Menendez, M., & Axhausen, K. W. (2021). How Many Cars in the City Are Too Many? Towards Finding the Optimal Modal Split for a Multi-Modal Urban Road Network. *Frontiers in Future Transportation*, *2*. https://doi.org/10.3389/ffutr.2021.665006

Lopez, P. A., Wiessner, E., Behrisch, M., Bieker-Walz, L., Erdmann, J., Flotterod, Y.-P., Hilbrich, R., Lucken, L., Rummel, J., & Wagner, P. (2018). Microscopic Traffic Simulation using SUMO. *2018 21st International Conference on Intelligent Transportation Systems (ITSC)*, 2575–2582. https://doi.org/10.1109/ITSC.2018.8569938

PTV Group. (2023). PTV Vissim. https://www.myptv.com/en/mobility-software/ptv-vissim

Pucher, J., & Buehler, R. (2017). Cycling towards a more sustainable transport future. *Transport Reviews*, *37*(6), 689–694. https://doi.org/10.1080/01441647.2017.1340234

Twaddle, H., Schendzielorz, T., & Fakler, O. (2014). Bicycles in Urban Areas. *Transportation Research Record: Journal of the Transportation Research Board*, *2434*(1), 140–146. https://doi.org/10.3141/2434-17

Wierbos, M. (2021). *Macroscopic Characteristics of Bicycle Traffic Flow* (Doctoral dissertation). Delft University of Technology.

Zhao, Y., & Zhang, H. (2017). A unified follow-the-leader model for vehicle, bicycle and pedestrian traffic. *Transportation Research Part B: Methodological*, *105*, 315–327. https://doi.org/10.1016/j.trb.2017.09.004